Toward an Active Contact Lens: Integration of a Wireless Power Harvesting IC

Jagdish Pandey, Yu-Te Liao, Andrew Lingley, Babak Parviz and Brian Otis

Department of Electrical Engineering, University of Washington, Seattle, WA

***Abstract*—The overarching goal of an active contact lens is to integrate sensing or display functionality onto a wearable device, enabling on-lens medical monitoring and heads-up displays. We present progress toward a wirelessly-powered active contact lens comprising a transparent polymer substrate, loop antenna, power harvesting IC, and a custom micro-LED. The fully integrated radio power harvesting and a power management system was fabricated in a 0.13 μm CMOS process and utilizes a small on-chip capacitor as an energy storage element to light up a micro-LED pixel. We have demonstrated wireless power transfer and LED intensity control using the custom IC and on-lens antenna.**

I. Introduction

Conventional contact lenses are designed for vision correction and aesthetics, but advances in low-power electronics and material processing make it possible to introduce additional functionality. Specifically, the realization of exceedingly small electronic, photonic, and sensing devices holds promise to turn contact lenses into functional microsystems for health monitoring or displaying information. For example, the cornea is composed of live cells that are in indirect contact with the blood serum. Thus many biomarkers that are found in the blood, such as glucose, are also detectable in the tear film. Additionally, with sophisticated optoelectronics and optical manipulation, such as vertical cavity surface emitting lasers (VCSELs) and micro-lens arrays, it may be possible to create on-lens displays [1]. Such a display could be useful as a heads-up display for pilots or gamers.

In order to realize this system, various subcomponents such as circuitry for power harvesting, display control, sensor read-out, and communication, together with an antenna, optoelectronic display pixels, and biosensors, must be integrated onto a thin, flexible, and transparent polymer substrate. Monolithic fabrication of such a device is not possible, so it is necessary to fabricate each subcomponent separately using unique and optimized processes and then use an appropriate assembly method to create the necessary mechanical and electrical connections.

Prior work [1] [2] has focused on developing an embedded sensor on a contact lens for medical monitoring. Leonardi et. al. have demostrated a embedded sensor on the contact lens for measuring the interocular pressure (IOP) for diagnosis and treatment of Glaucoma [2]. However, the device does not incorporate a telemetry chip or antenna, both of which are critical components of a complete system.

In this paper, we demonstrate a wirelessly-powered micro-LED embedded in the active lens using a custom antenna and fully integrated storage capacitor on a transparent substrate. Like an RFID system, power is supplied wirelessly, avoiding the need for large capacitors and batteries.

The rest of the paper is organized as follows. Section II presents system feasibility analyses. The lens fabrication process including the antenna design is presented in section III. Section IV describes the design of the custom chip containing the power harvesting, energy storage and power management circuits. Section V presents measurement results and conclusions are presented in Section VI.

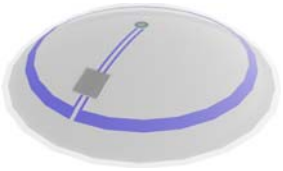

Fig. 1. A conceptual drawing of the active contact lens.

II. System Feasibility

In this section, we explore the feasibility of wirelessly powering a micro-LED using a thin film custom antenna on the lens. We derive the constraints on the CMOS rectifier design and impedance matching, and calculate a maximum theoretical distance of operation with a 1 W RF power source.

A. Energy calculations

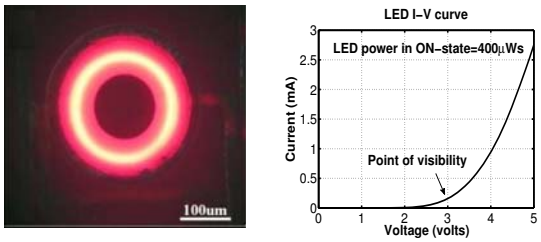

Fig. 2. The lit-up custom LED [1] and its $I-V$ characterstic.

In [6], we present a custom LED. As shown in Fig. 2, the micro-LED turn-on voltage is 3 V with a 400 μW power consumption. If we assume 500 mV of maximum allowable ripple ($V_2 = 3.5\,V$ and $V_1 = 3.0\,V$) on the DC voltage, and

978-1-4244-4918-7/09/$25.00 ©2009 IEEE

a $1\,\mu$s ripple period, the size, C, of the storage capacitor is given by

$$\frac{1}{2}CV_2^2 - \frac{1}{2}CV_1^2 = P_{LED} \cdot T \quad (1)$$

where P_{LED} is the LED power consumption and T is the ripple period. (1) leads to a 246 pF storage capacitor which is very large considering the fact that tens of such pixels need to be supplied by the on-chip storage capacitor. The size of storage capacitor and therefore the total stored energy is constrained by the fact that the maximum allowable size of the chip is $\approx 500 \times 500\,\mu\text{m}^2$ due to the curvature (≈ 7.9 mm [3]) and thickness ($\approx 200\,\mu$m [4]) of the contact lens. Fortunately, humans cannot perceive fluctuations above approximately 60 Hz in light sources, and as a consequence duty cycling can be used to keep the LED appear continuously activated. We employ 3% duty cycling at 1 MHz frequency. With 3% duty-cycling, the average power dissipation of the LED is only $12\,\mu$W. For 500 mV of maximum allowable ripple, this leads to a 7.4 pF storage capacitance value. Given that integrated capacitors of the order of a nF can be realized, 7.4 pF of storage capacitor per pixel is commensurate with our goal of eventually powering tens of such pixels wirelessly.

B. Range calculations

In order to calculate the maximum range of operation, we need to consider the minimum input power to the antenna and maximum allowed transmit power in 2.4 GHz band, the choice of ISM band for the wireless link. We primarily consider two constraints on this minimum input power: the antenna/rectifier power efficiency, and the input voltage amplitude to the rectifier which in turn is constrained by the LED turn-on voltage, rectifier threshold and impedance matching to the antenna.

For a carrier frequency of 2.4 GHz and a maximum diameter of on-lens loop antenna of 1 cm, the ratio of the circumference of the antenna to the wavelength is about 0.25. Thus the antenna can be loosely approximated as a small loop antenna. The radiation resistance of a small loop antenna is given by [5]

$$R_r \approx 32,000 \left(\frac{A}{\lambda^2}\right)^2 \quad (2)$$

where A is the area of the loop antenna and λ is the wavelength of the incident RF wave. If the metal thickness is several times the skin depth and since the RF waves impinge the thin-film antenna only from the top, we can approximate the antenna ohmic losses by [5]

$$R_{ohmic} \approx R_s \left(\frac{2\pi r}{t+w}\right), \text{with } R_s = \sqrt{\frac{\pi f \mu}{\sigma}} \quad (3)$$

where r, t, and w are loop radius, thickness and width of the antenna trace respectively, and μ is the permeability of free space. R_s is the surface resistance of the trace and σ is the conductivity of trace metal (gold). The antenna efficiency is defined as

$$\eta = \frac{R_{rad}}{R_{rad} + R_{ohmic}} \quad (4)$$

Using these approximations, with $f = 2.4$ GHz, loop radius $r = 5$ mm, wire width $w = 200\,\mu$m, thickness $t = 10\,\mu$m, conductivity $\sigma = 4.52 \times 10^7\,\Omega^{-1}\text{m}^{-1}$, we can evaluate $R_{ohmic} = 2.17\,\Omega$ and $R_{rad} = 0.81\,\Omega$. This leads to theoretical antenna efficiency of 27.2%.

If we assume 10% efficiency of the rectifer and $12\,\mu$W power consumption of the pixel, the input power to the chip should be $120\,\mu$W. Assuming maximum power transfer and 25% antenna efficiency, the minimum incident power ($P_{Rx,min}$) on the antenna must be approximately 1 mW (0 dBm).

We now consider the constraint of rectifier input voltage, resulting from the output voltage of $\sim$3 V and impedance matching.

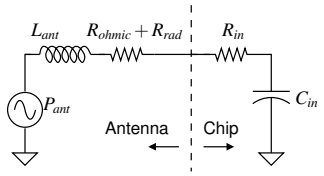

Fig. 3. Conjugate impedance matching between the antenna and the IC.

Fig. 3 shows the equivalent circuit model of the antenna and the chip. The small loop antenna is approximated as a power source with inductive source impedance at 2.4 GHz. For maximum power transfer, the chip input impedance is conjugate matched to the antenna impedance. Due to fabrication constraints, we have a high ohmic loss, $R_{ohmic} \sim 7\,\Omega$. In our design, $R_{ohmic} + R_{rad} \approx 7.5\,\Omega$, $L_{ant} = 3$ nH, $R_{in} = 7\,\Omega$ and $C_{in} = 1.4$ pF. The quality factor, Q_{in} of the chip input impedance, defined as $1/\omega R_{in} C_{in}$, is approximately 6.5. Assuming conjugate input matching, the available input voltage amplitude V_{in} is given by

$$\frac{P_{ant}}{2} = \frac{V_{in}^2}{2 \cdot R_s(1 + Q_{in}^2)} \quad (5)$$

where P_{ant} is the antenna source power as shown in Fig. 3. For rectifier threshold voltage of $V_{th} = 750$ mV, $R_{in} = 7\,\Omega$, $Q = 6.5$, P_{ant} evaluates to be 1.85 mW. Assuming 25% antenna efficiency, this requires 7.4 mW (8.7 dBm) of minimum incident power $P_{Rx,min}$. This is the deciding constraint on $P_{Rx,min}$ which we use in the calculations below to evaluate the maximum range of operation.

Assuming line-of-sight communication,

$$P_{Rx} = P_{Tx} + G_{Tx} - L_{FS} + G_{Rx} \quad (6)$$

where P_{Rx} and P_{Tx} are the received and transmit powers (dBm) respectively. G_{Rx} and G_{Tx} are the received and transmit antennae gains (dBi) respectively. L_{FS} represents the free path loss given by [5]

$$L_{FS}(\text{dB}) = 10 \cdot \log_{10}\left(\frac{4\pi df}{c}\right)^2 \quad (7)$$

$$= 20\log_{10}(d) + 20\log_{10}(f) - 147.56 \quad (8)$$

Assuming 10 dBi gain for transmit antenna and an isotropic receive antenna, P_{Rx}=8.7 dBm and 1 W (P_{Tx}=30 dBm) hand-held source (maximum transmit power in 2.4 GHz band as allowed by FCC regulations) the range d can be calculated to be 36.5 cm, which satisfies the operational range requirement for our application. However, it must be stated that losses due to suboptimal matching, interface reflections, and absorption in the eye have not been taken into account and could substantially degrade performance. For the bio-safety requirements, we turn to the IEEE guidelines. The IEEE standard C95.1 approved radiation level for biological safety is approximetely 8 mW/cm^2 at 2.4 GHz [7].

III. Lens Fabrication

First, in order to withstand basic microfabrication, the substrate material must be able to resist temperatures up to 75°C, associated with photolithography and metal evaporation, and also common solvents such as acetone and isopropyl alcohol, which eliminates most state-of-the-art contact lens materials. The substrate must be clear as to not obstruct the wearer's vision. Polyethylene terephthalate (PET) is a clear polymer which does not dissolve in common solvents used in microfabrication, nor does it warp substantially at relevant temperatures. Although biocompatible, specifically oxygen permeability, is a concern, the primary focus of this work is to determine feasibility at a system level. Therefore, we use a 100 μm thick sheet of PET as the lens substrate.

A modified, low temperature positive photolithography using AZ4620 (Microchem) is used to create patterns for metal deposition and lift-off. The metallization is Cr/Ni/Au (30 nm, 80 nm, 1 μm) to provide good adhesion, solderability, and low resistance interconnects with a single evaporation run. For the antenna, it would be beneficial to deposit a metal trace several times the thickness of the skin depth to increase efficiency. However, in order to simplify processing the same metallization was used for the pads, interconnects, and the antenna. Negative lithography is used to deposit permanent a transparent, biocompatible negative photoresist (SU-8, Microchem), for electrical insulation and to create wells in which to place components.

The IC was implemented in the IBM 130 nm process. For the micro-LEDs, aluminum gallium arsenide was chosen because of its efficient emission and established usage as an optoelectronic material. Details of the LED design, fabrication, and initial testing are provided in [6].

Due to size and vision constraints (i.e. 1 cm diameter and a ~5 mm diameter aperture for the pupil), the most practical antenna is a loop configuration. We simulated the antenna using the cross section of [4(a)] and an antenna diameter of 0.9 cm.

IV. Radio Power Harvesting IC

Fig. 5 shows the architecture of the CMOS prototype chip containing the power harvesting, storage capacitor and power management circuitry. It houses 450 pF of integrated storage capacitance. Some of the important challenges in making

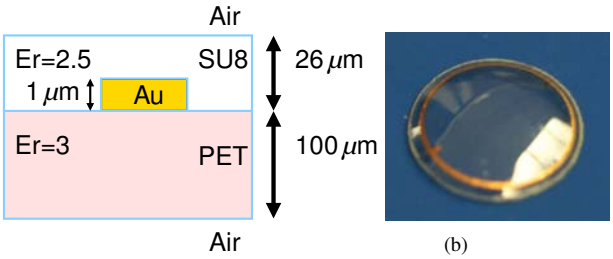

Fig. 4. (a) Stack-up of the contact lens assembly. (b) Image of a molded contact lens with loop antenna.

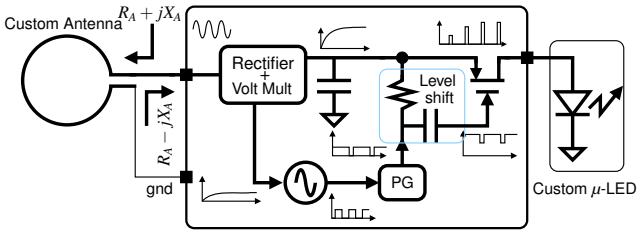

Fig. 5. Architecture of the custom chip.

an integrated RF power harvesting system are designing an efficient rectifier, an intelligent, robust power management system, and realizing a high-density on-chip storage capacitor. To avoid junction and oxide breakdown of the transistors in our technology (0.13 μm CMOS) we chose the rectifier scheme shown in Fig. 6. We chose a CMOS process that provides low threshold transistors for enhanced rectifier sensitivity. The diodes are realized using PMOS transistors with the body terminal tied to the source in order to eliminate the body effect.

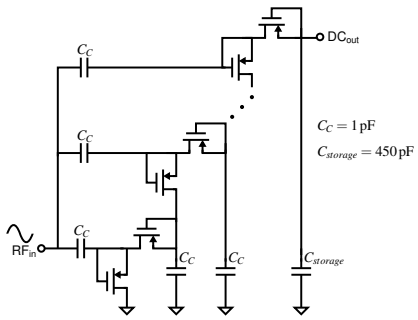

Fig. 6. Eight-stage rectifier design using low-V_t PMOS devices.

The optimal number of stages in the multiplying rectifier was determined by considering the trade-off between its power efficiency, output voltage, input impedance for matching and the micro-LED load (capacitor charging time). We have chosen eight stages which provides approximately $8 \cdot (V_{RF} - V_t) \approx$ 3.6 V of DC output for 750 mV RF input and 300 mV threshold voltage.

For maximum energy storage on the capacitor, the DC voltage must be maximized under the breakdown voltage constraint (10 V). However, the large number of stages required

for achieving this high voltage leads to increased capacitor charging time, degraded quality factor of the input impedance and unreasonable values for the antenna impedance matching [8]. Another important aspect of the rectifier design is the choice of coupling capacitor (C_c). It should be much larger than the parasitic capacitance of the MOS diodes but should be small enough to facilitate input matching and higher quality factor of the input impedance of the chip (for passive voltage gain). For our application, 1 pF was found to be a good compromise. For the application of on-lens display system using our custom LEDs, the optimal number of stages was found to be eight.

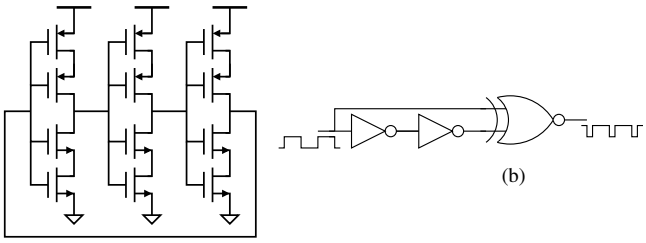

(a) (b)

Fig. 7. (a) Low leakage ring oscillator using high-V_t stacked transistors. (b) Frequency doubling pulse generation circuit.

A robust power management circuit is absolutely crucial for ensuring reliable circuit functionality in the face of scarce power resources on chip. The power management circuit allows powering the LED for approximately 3% of the time by modulating the 3.3 V PMOS switch. The on-chip ring oscillator shown in Fig. 7(a) derives its power supply (∼1 V) from the second stage of the cascaded rectifier. Each inverter in the 3-stage oscillator uses stacked high-V_t devices for low leakage and low-power of operation (∼500 nW at 1 MHz). The frequency doubling pulse generation circuit shown in Fig. 7 generates an active low pulse at each transition of the oscillator output of approximately $0.015/f$ long duration where f is the frequency of the ring oscillator. This means that the pulse generator effectively generates active low pulses of 3% duty cycle at a frequency $2f$. The level shifter circuit uses the output of rectifier to upconvert the active-low pulses with active high and active low being 3.5 and 2.5 V respectively.

The difficulty in realizing very small high quality tank circuits on the plastic substrate and the extremely small size of the chip prevents any passive impedance matching tank circuit for passive voltage gain. This results in loss of sensitivity of the rectifier.

V. Measurement Results

Fig. 8 shows the measured efficiency of the rectifier system while power the LED at 3 V. Fig. 9(a) captures the waveforms, V_{LED} and $V_{Level\text{-}Shifter}$ at the drain and gate terminals of the PMOS duty-cycle control switch respectively. Fig. 9 shows the chip micrograph ($450\times480\,\mu m^2$).

Using a 2 GHz dipole antenna at the RF reader, we have demonstrated an LED turn-on range of approximately 2 mm

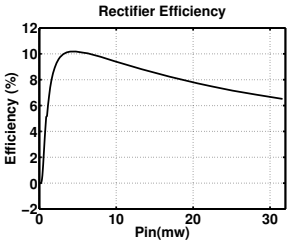

Fig. 8. Measured efficiency (%) of the power harvesting system

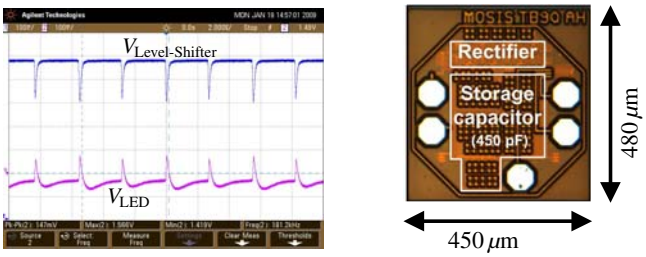

(a) (b)

Fig. 9. (a) The level-shifted duty-cycled pulse and the voltage pulses applied to the μ-LED. (b) Chip micrograph.

using a 25 dBm RF source. Therefore, we are operating well within the near field of the dipole antenna. The poor range of operation can be attributed to antenna efficiency, suboptimal matching, and low dipole antenna directivity. However, as determined in Section II, with a modified antenna fabrication process, transmit antenna, and improved matching, we expect far field operation.

VI. Conclusion

We have taken the first steps towards a functional active contact lens. We have demonstrated that a small loop antenna connected through an power harvesting IC can power a micro-LED on a transparent substrate. Through optimization of the antenna and impedance matching, we hope to create a system with a range of several centimeters.

Acknowledgment

The authors thank Microsoft, and UW Technology Gap Innovation Fund for partial support of this project.

References

[1] Ho, H. et al, "Contact lens with integrated inorganic semiconductor devices," *IEEE International Conference on MEMS, 2008* Jan. 2008
[2] M. Leonardi et al, "A soft contact lens with a MEMS strain gage embedded for intraocular pressure monitoring," *International Conference on Transducers* vol. 2 2003
[3] H. Patel et al, "Identifying relationships between tomography-derived corneal thickness, curvature, and diameter," *Eye*, vol. 23, pages 270-278, February 2008.
[4] Anthony Phillips et al Contact Lenses. 5th ed. New York: Elsevier, 2007.
[5] Stutzman et al, "Antenna Theory and Design," Wiley Publications
[6] E. Saeedi et al, "Self-assembled inorganic micro-display on plastic," IEEE International Conference on MEMS, Pages(s): 755-758, 21-25 Jan. 2007
[7] "IEEE Standard C59.1"
[8] T. Le et al, "Efficient far-field radio frequency energy harvesting for passively powered sensor networks," *IEEE JSSC* vol. 43, Issue 5, Page(s): 1287-1302, May 2008